

Catalytic Epoxidation of Olefins with Graphene Oxide Supported Copper (Salen) Complex

Qingshan Zhao, Chan Bai, Wenfeng Zhang, Yang Li, Guoliang Zhang, Fengbao Zhang, and Xiaobin Fan*

State Key Laboratory of Chemical Engineering, Key Laboratory for Green Chemical Technology, School of Chemical Engineering & Technology, Collaborative Innovation Center of Chemical Science and Engineering, Tianjin University, Tianjin 300072, China

 *Supporting Information*

ABSTRACT: Immobilization of metal complexes on solid supports is an efficient approach to remedy the drawbacks of homogeneous catalysis. In this study, an *in situ* strategy of synthesis and immobilization of a copper (salen) complex onto graphene oxide (GO) support has been developed. To provide the salen ligands, GO was covalently modified with an aminosilane, followed by condensation with salicylaldehyde. The copper (salen) complex was subsequently synthesized and simultaneously immobilized onto the GO surface with a designed tetrahedral chelate structure. The immobilized copper (salen) complex [Cu(salen)-f-GO] kept the two-dimensional sheetlike character of GO and was demonstrated to be highly effective for the epoxidation of olefins. It could be readily reused for successive twelve times without discernible activity and selectivity deterioration, which displays potential for practical applications.

1. INTRODUCTION

Transition metal complexes are one of the most useful and powerful catalysts for industrial processes. However, the practical applications of homogeneous metal complexes are hampered by their high costs with problems of separating from the reaction mixtures. Therefore, designing heterogenized metal complex catalysts is of great interest for economic and environmental reasons in recent years.^{1–4} By being immobilized on insoluble solid materials, the high cost and toxic metal complex catalysts can be easily recovered from the reaction mixtures and ready for reuse.⁵ Various approaches to obtain an ideal heterogenized metal complex catalyst have been developed. Among them, covalent binding of metal complexes onto the support through a ligand spacer is the most efficient and commonly used strategy. Thus, a wide range of matrixes has been developed for covalent attachment of metal complexes, such as inorganic mesoporous materials,^{3,6} organic polymers,^{7,8} and dendrimers.⁹ However, the potential and utility of these immobilized catalysts are closely related to the structural nature of the support.¹⁰ For instance, the presence of metal complexes in a porous matrix with abundant micropores might cause serious diffusion resistance, and the catalytic processes may fall into a mass transfer controlled region. Furthermore, the ligand spacer plays a crucial role on the catalytic performance.¹¹ The electronic properties and steric circumstances around the metal center would be affected when the complex is directly immobilized through axial coordination, and weak coordination interaction may cause heavy metal leaching in the application processes. In fact, immobilized metal complex catalysts often suffer from inferior catalytic activity and metal leaching as well as high preparation complexity. Therefore, searching and developing new efficient supports and strategies are still an urgent task.

Recently, graphene and graphene oxide (GO) with interesting two-dimensional structures and unique properties^{12–15} have emerged as ideal supports for a variety of

catalytic species.^{16–21} Besides the availability of surface functionalization,^{22–26} their two-dimensional structures not only allow excellent dispersion of the catalytic species but also facilitate mass transfer in the reaction processes. Reactive species can readily access the active sites with limited mass transfer resistance. Therefore, remarkable catalytic performance of graphene or GO supported catalysts have been observed. In our previous work, we have successfully immobilized a commercial rhodium catalyst [RhCl(PP₃)₃] onto GO through a simple coordination attachment method and demonstrated its efficiency in the hydrogenation of cyclohexene.²⁷ Herein, we developed an *in situ* strategy of synthesis and immobilization of a copper (salen) complex onto GO support. It was found that the immobilized copper (salen) complex [Cu(salen)-f-GO] with a designed tetrahedral chelate structure not only showed superior catalytic activity for the epoxidation of olefins but also exhibited outstanding stability even after intensive reuse, which displays its potential for practical applications.

2. EXPERIMENTAL SECTION

2.1. Materials. The graphite powder was purchased from Sigma-Aldrich Chem. Co. (USA). 3-(Aminopropyl) trimethoxysilane (APTMS, 97%) salicylaldehyde (99%), copper(II) nitrate trihydrate (Cu(NO₃)₂·3H₂O, 99%), styrene (99%), α -methylstyrene (99%), norbornylene (99%), cyclohexene (99%), cyclooctene (99.5%), 1-octene (98%), acetonitrile (99%), and *tert*-butyl hydroperoxide (*tert*-BuOOH, 70% solution in water) were purchased from Aladdin Reagent Co. (Shanghai, China). All other materials were commercially available and used without further purification.

Received: January 2, 2014

Revised: February 19, 2014

Accepted: February 21, 2014

Published: February 21, 2014



2.2. Test Methods. Fourier transform infrared (FTIR) spectra were performed on a Nicolet Nexus FTIR spectrometer using KBr pellets. X-ray photoelectron spectroscopy (XPS) measurements were carried out on a PHI 1600 spectrometer (Perkin-Elmer). Raman spectra were measured with a NTEGRA Raman spectrometer (NT-MDT) with an excitation laser wavelength of 514 nm. Electron paramagnetic resonance (EPR) spectra were obtained using an EMX Bruker spectrometer at 150 K. Scanning electron microscopic (SEM) images and energy dispersive X-ray spectroscopy (EDS) analysis were recorded using a Hitachi S-4800 Instrument. Transmission electron microscopic (TEM) images were recorded using a JEM-2100F transmission electron microscope operating at 200 kV. The loading content and leaching of copper were determined by inductively coupled plasma optical emission spectroscopy (ICP-OES, Vista-MPX). The catalytic results were measured by Agilent 6890N gas chromatography (GC) using a GC-FID system.

2.3. Preparation of GO and APTMS-f-GO**.** GO was prepared and purified by the Hummers method.²⁸ The as-prepared GO (8.0 mg mL⁻¹, 25 mL) was dispersed in 150 mL of ethanol and loaded in a 250 mL round-bottom flask, followed by stirring and ultrasonication the dispersion for 0.5 h (25 W, 40 kHz). Subsequently, APTMS (369.6 mg, 2.0 mmol) was dropwise added into the suspension. The mixture was stirred and refluxed for 6 h. After cooling to room temperatures, the prepared APTMS-f-**GO** was filtrated and washed with absolute ethanol and water three times, respectively. A black solid was obtained after a freeze-drying procedure.

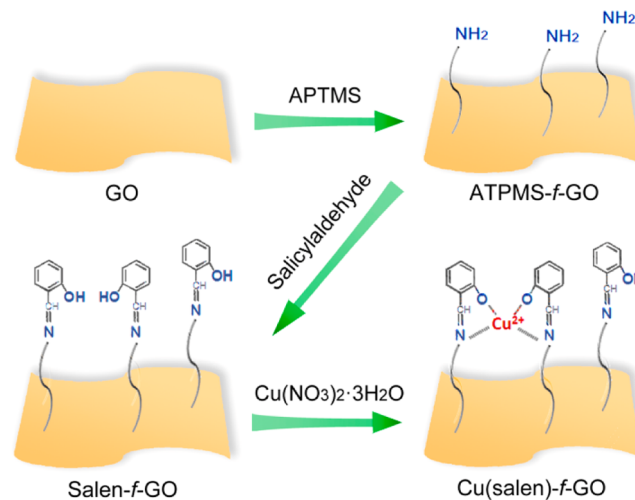
2.4. Synthesis of Cu-f-GO**.** The as-prepared APTMS-f-**GO** was dispersed in 60 mL of absolute ethanol again. Excess salicyaldehyde (370.0 mg, 3.0 mmol) and a few drops of acetic acid as an accelerator were added into the suspension. After refluxing for 5 h, black solid was achieved by filtering the mixture and washing with methanol twice. Finally, the solid was mixed with Cu(NO₃)₂·3H₂O (488.1 mg, 2.0 mmol) in methanol and stirred for 12 h at room temperatures. The resulting mixture was filtered and washed with methanol, ethanol, and water three times, respectively, followed by freeze-drying.

2.5. Catalytic Epoxidation Reactions. The catalytic reactions were conducted in a 25 mL two-neck glass flask. 10.0 mmol of the substrate and 60 mg of Cu(salen)-f-**GO** were dispersed in 12 mL of acetonitrile, and *tert*-BuOOH (2.57 g, 20 mmol) was dropwise added into the solution. The mixture was equilibrated to 80 °C using an oil bath and stirred for 12 h. At the stated time, samples were taken from the reaction mixture and analyzed by GC. Repeated experiments were carried out for averaging catalytic data. For the recycling experiments, the reactions were carried out under the above conditions. After each run, the used catalyst was recovered from the reaction mixture by careful filtration and reused in sequential runs after washing with acetonitrile twice.

3. RESULTS AND DISCUSSION

3.1. Synthesis and Characterization of Cu(salen)-f-GO**.** The copper (salen) complex was immobilized onto GO support by an *in situ* strategy as illustrated in Scheme 1. In brief, GO was first covalently modified with an aminosilane [3-(aminopropyl)trimethoxysilane, APTMS] through a silylation reaction with the surface hydroxyl groups.²⁹ Salicylaldehyde was sequentially introduced to the silane terminal by condensation

Scheme 1. Illustration for the Synthetic Methodology of Cu(salen)-f-GO****



with the apical amine groups, providing bidentate ligands for anchoring of copper ions. The copper (salen) complex was subsequently synthesized and simultaneously immobilized onto the GO surface.

Fourier transform infrared (FTIR) spectra of the pristine GO, APTMS modified GO (APTMS-f-**GO**), and Cu(salen)-f-**GO** are shown in Figure 1. Comparison studies on GO and

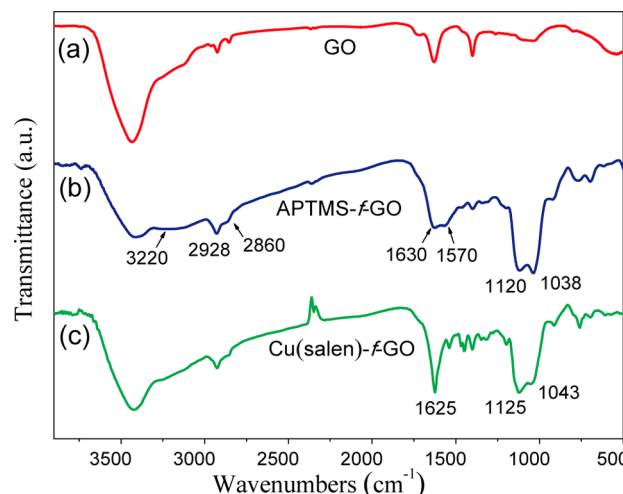


Figure 1. FTIR spectra of (a) GO, (b) APTMS-f-**GO**, and (c) Cu(salen)-f-**GO**. Note that the bands at around 3450 and 1400 cm⁻¹ partially ascribe to absorbed water. In the spectra of GO and APTMS-f-**GO**, the bands at about 1630 cm⁻¹ is attributed to in-plane vibrations of C=C bonds.

APTMS-f-**GO** reveal additional strong bands at 1120 and 1038 cm⁻¹ corresponding to characteristic absorption of Si-O bonds formed through the silylation process.²⁹ The new doublet at 2928 and 2860 cm⁻¹ assigned to stretching vibrations of C-H bonds³⁰ and the vibrations of N-H bonds³¹ at around 3220 and 1570 cm⁻¹ further verify the introduction of the aminosilane chains. Upon condensation with salicyaldehyde, a significant decrease can be observed for the N-H absorbance range, whereas an enhanced sharp band near 1625 cm⁻¹ associated with stretching vibrations of C≡N appears (Figure 1c). The multipeaks in the 1400–1600 cm⁻¹

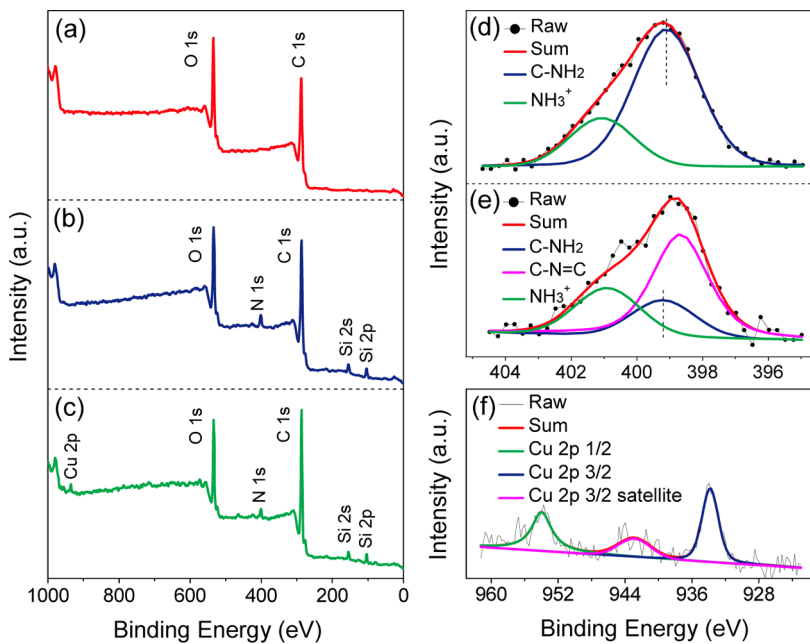


Figure 2. Full range XPS spectra of (a) GO, (b) APTMS-*f*-GO, and (c) Cu(salen)-*f*-GO. N1s XPS spectra of (d) APTMS-*f*-GO and (e) Cu(salen)-*f*-GO. (f) Cu 2p XPS spectrum of Cu(salen)-*f*-GO.

region present characteristic absorption from the benzene rings of salicyldehyde. Notice that free C=N vibrations are generally located at around 1640 cm^{-1} , and this red shift ($\sim 15\text{ cm}^{-1}$) to relatively lower frequency might be attributed to coordination interaction with the copper ions. Similar phenomenon has been observed in related reports.³² These results confirm the successful binding of salen ligands and anchoring of copper complexes onto the GO surface.

As shown in the X-ray photoelectron spectroscopy (XPS) spectra of GO, APTMS-*f*-GO, and Cu(salen)-*f*-GO (Figure 2a-c), Si and N signals can be clearly observed after the silylation modification, with additional Cu signal in Cu(salen)-*f*-GO. Compared with the C1s spectrum of GO, APTMS-*f*-GO exhibits an obvious decrease of the C–O–C and C–OH band at around 286.5 eV,³³ while a new band at 101.8 eV attributed to Si–O³⁴ emerges in the Si 2p spectrum (Figure S1, Supporting Information). This indicates the silylation reaction between silanol and surface hydroxyl groups. N1s XPS spectra of APTMS-*f*-GO and Cu(salen)-*f*-GO reveal that a considerable amount of N–H was converted into N=C (398.6 eV) after condensation with salicyldehyde, and the N–H band shifts from 399.10 to 399.25 eV which should be caused by the donor–acceptor interaction of nitrogen atom with the central copper ions (Figure 2d, e).^{35,36} Cu 2p XPS spectrum of Cu(salen)-*f*-GO shows two typical bands at 933.9 and 953.8 eV which corresponds to the bonding energy of copper(II) (Figure 2f). Meanwhile, a Cu 2p_{3/2} satellite peak at 943.0 eV emerges, demonstrating the coordination interaction between the salen ligand and the copper center.³⁷ Considering the limitation of surface characterization by XPS, the copper content is determined by inductively coupled plasma optical emission spectroscopy (ICP-OES), and the copper content was detected to be 0.67 wt % (0.10 mmol g⁻¹).

The chemical and structural changes in the obtained materials can be also reflected in the Raman spectra (Figure 3). Raman spectra of GO, APTMS-*f*-GO, and Cu(salen)-*f*-GO illustrate the presence of two characteristic bands that correspond to the disorder induced *D* band and *G* band

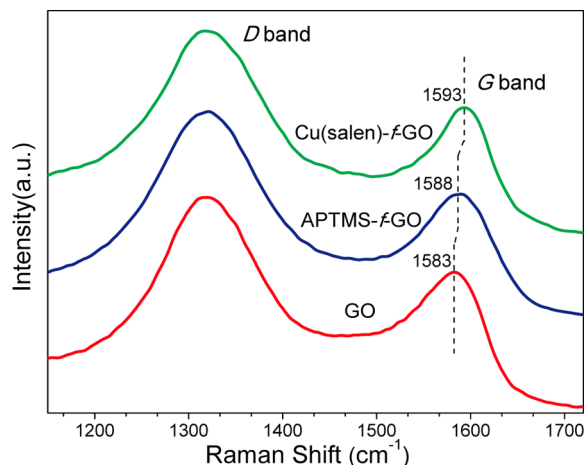


Figure 3. Raman spectra of GO (red), APTMS-*f*-GO (blue), and Cu(salen)-*f*-GO (green).

associated with the vibrations of sp² bonded carbon networks.³⁸ The intensity ratio of *D* and *G* band (I_D/I_G) displays an obvious increase from 1.78 to 1.98 and 2.16, and the increased change in disorder is probably due to the formation of more edges and defects during the reaction processes. Anchoring of the aminosilanes and copper complexes onto the GO surface might also lead to the increase in intensity ratio.³⁹ The position of the *D* band is almost the same before and after the chemical modifications. However, the *G* band shifts from 1583 to 1588 cm^{-1} after the silylation reaction, with a further blue shift to 1593 cm^{-1} for Cu(salen)-*f*-GO. This upshift might be attributed to the gradually increased compressive local stress caused by the covalent binding chains.⁴⁰ This phenomenon may also suggest an effective charge transfer^{41,42} from GO to the aminosilane and the copper (salen) complex.

To provide direct evidence for the immobilization of the copper (salen) complex with the designed structure, electron paramagnetic resonance (EPR) is employed to characterize the

steric configuration of Cu(salen)-*f*-GO. A typical EPR spectrum of magnetically diluted copper species can be seen in Figure 4, which indicates the presence of the copper (salen)

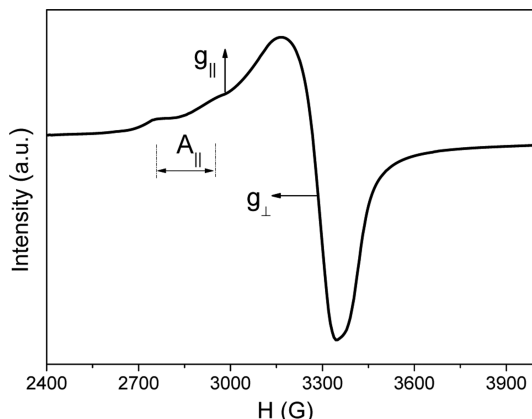


Figure 4. EPR spectrum of Cu(salen)-*f*-GO recorded at 150 K.

complex. The hyperfine coupling arising from the central copper ions (^{63}Cu , $I = 3/2$) can also be resolved, although the feature was not that clear due to intermolecular interactions. The principle g_{\parallel} and g_{\perp} of Cu(salen)-*f*-GO are calculated to be 2.28 and 2.07, respectively. The A_{\parallel} value is calculated to be 190 G. Typically, copper complexes with $g_{\parallel} > g_{\perp} > 2.0023$ suggest that the unpaired electron occupies the $d_{x^2-y^2}$ d orbital, which is the characteristic for a tetragonal elongated coordination environment of the copper center.⁴³ The results are in accordance with copper systems of tetragonal planar structures.⁴⁴ As designed, the EPR result confirms the tetrahedral chelate arrangement of the copper (salen) complex immobilized on GO.

Scanning electron microscopy (SEM) and transmission electron microscopy (TEM) images present the microstructure and morphology of the samples. (Figure 5). Compared with the two-dimensional planar GO, APTMS-*f*-GO and Cu(salen)-*f*-GO keep the sheetlike structure with more crumpling features which may be induced by the chemical modifications (Figure 5a-c). TEM images show similar characteristics and verify that the microstructure of GO is not destroyed through the modification processes (Figure 5d-f). Further studies on quantitative energy dispersive X-ray spectroscopy (EDS)

mapping show that Si, N, O, and Cu elements can be homogeneously distributed on the whole GO surface, implying a uniform immobilization of the copper (salen) complexes (Figure S2, Supporting Information). Photographs of GO, APTMS-*f*-GO, and Cu(salen)-*f*-GO reveal the samples are well dispersed in the solvent (Figure S3, Supporting Information). Thus, the immobilized catalyst can be fully extended and displays a sheetlike morphological feature in the reaction media, which serves as a versatile platform for the access and leaving of the reactive species with the surface catalytic active sites.⁴⁵

3.2. Catalytic Epoxidation Reactions. Since the immobilized catalyst has been successfully prepared, its catalytic performance was evaluated through the epoxidation of olefins using *tert*-BuOOH as the oxidation. A study was first made of the catalytic behavior in the epoxidation of styrene. As shown in Figure 6, the conversion and yield increased with reaction time

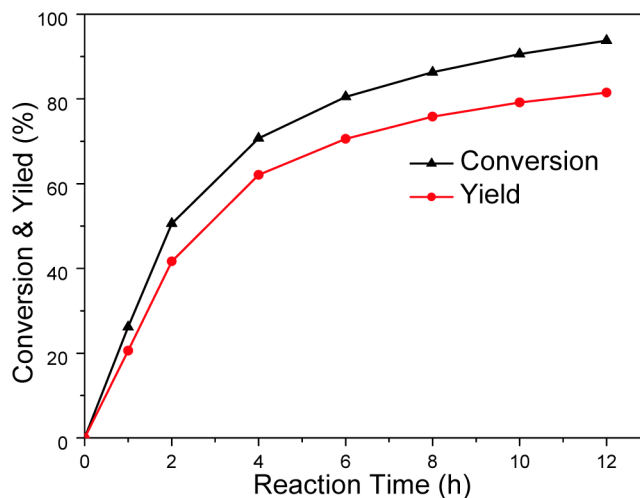


Figure 6. Curve of conversion and yield versus reaction time for styrene epoxidation.

and reached to 94.5% and 81.8% in 12 h, with a turnover frequency (TOF) of 413.7 h^{-1} . The selectivity was 86.6%, and the main byproduct was detected to be benzaldehyde. In order to investigate the universality of the catalyst, further studies on more olefins were performed. As summarized in Table 1, α -

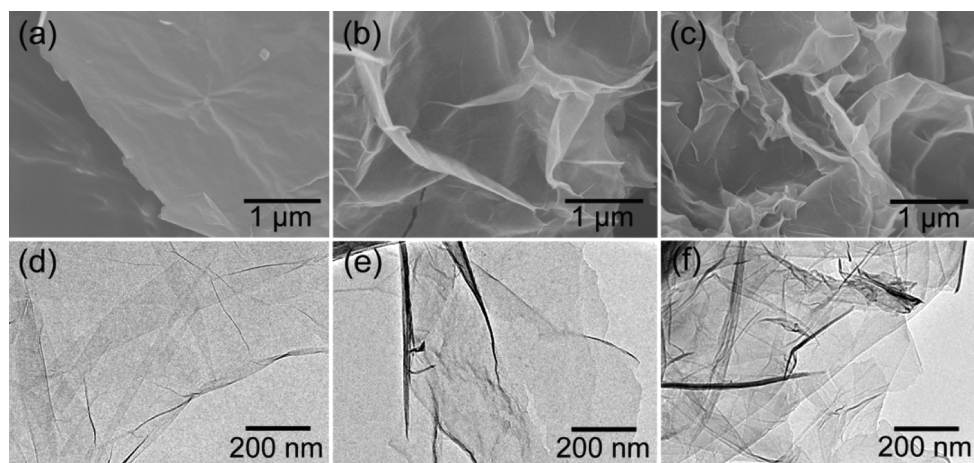


Figure 5. SEM and TEM images of (a), (d) GO; (b), (e) APTMS-*f*-GO; and (c), (f) Cu(salen)-*f*-GO.

Table 1. Catalytic Epoxidation of Olefins by Cu(salen)-*f*-GO^a

Entry	Substrate	Conversion (%)	Yield (%) ^b	Final TOF (h^{-1}) ^c
1		94.5	81.8	124.6
2		91.7	77.4	120.8
3		99.0	98.3	130.5
4		75.3	65.5	99.3
5		52.8	43.6	69.6
6		42.1	31.5	55.5

^aGeneral conditions: Substrate (10 mmol), Cu(salen)-*f*-GO (60 mg), *tert*-BuOOH (2.57 g), acetonitrile (12 mL), 80 °C, 12 h.

^bCalibrated yields determined by GC. ^cFinal turnover frequency = mol converted/mol of active sites/reaction time.

methylstyrene showed a conversion of 91.7% and yield of 77.4%, with a final TOF of 120.8 h^{-1} . The epoxidation of cyclic bridge norbornene proceeded smoothly under the same conditions. The conversion and yield reached up to 99.0% and 98.3%, respectively. The final TOF was calculated to be 130.5 h^{-1} . As comparison, cyclohexene showed slightly lower activity, with a conversion of 75.3% and yield of 65.5%. For cyclooctene, the conversion and yield were determined to be 52.8% and 43.6%, respectively, whereas the chain aliphatic 1-octene gave only 42.1% conversion and 31.5% yield within the same time. The relatively lower conversion of the cyclo and long-chain olefins is most likely attributed to the increased steric hindrance raised from the cyclo and chain structure as well as the higher ring strain. These catalytic results revealed that Cu(salen)-*f*-GO was an efficient catalyst for the epoxidation of olefins.

After the reaction, the solid catalyst could be easily recovered from the reaction mixture by direct filtration or centrifugation and ready for reuse after washing with acetonitrile twice. So the reusability of Cu(salen)-*f*-GO was tested through the epoxidation of styrene. As summarized in Figure 7, Cu(salen)-*f*-GO showed excellent stability upon reuse. The catalyst could maintain its high activity and selectivity for at least successive twelve cycles without discernible activity and selectivity deterioration. After each run, metal leaching was examined by ICP analysis, and no detectable copper presented, revealing the high stability of the catalyst. Compared with our prior strategy,²⁷ the prepared catalyst shows excellent catalytic activity and superior reusability. So to further investigate effect of the support and the designed structure on the catalytic behavior, control experiments were carried out. Styrene was chosen as a standard substrate, and the experiments were conducted under the above conditions (see the Supporting Information for details). The catalytic results were summarized

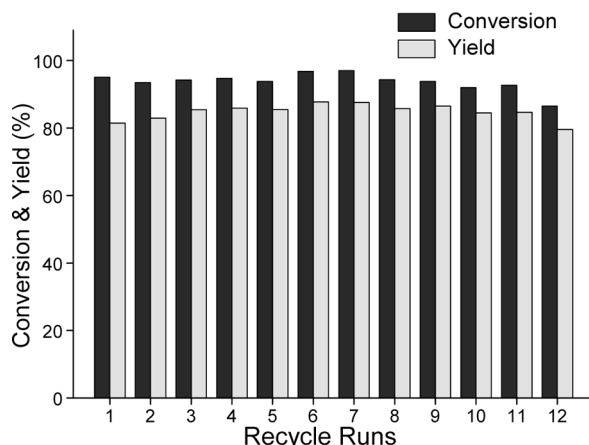


Figure 7. Catalyst recycling runs for styrene epoxidation.

in Figure S4 (Supporting Information). The pristine GO and APTMS-*f*-GO showed hardly any catalytic activity for styrene epoxidation. When the copper salt [Cu(NO₃)₂] was directly immobilized through axial coordination onto APTMS-*f*-GO (the sample was named as Cu-*f*-GO), only 17% conversion and 15% yield were obtained. The homogeneous Cu(NO₃)₂ could achieve comparable conversion of 86%, but lower selectivity (70%) compared with the immobilized catalyst.

In general, excellent catalytic results should be achieved when the reaction is catalyzed by the homogeneous copper salt. However, formation of inactive dimers or aggregates cannot be totally avoided in the reaction mixture, which may shield the catalytic active sites⁴⁶ and affect its catalytic performance. As to the immobilized copper system, given the site isolation effect by immobilization,^{47,48} the copper catalytic sites can be separated from each other and keep the high efficiency throughout the whole catalytic process. On this basis, the superior catalytic performance of Cu(salen)-*f*-GO also lies in the fact that it can be easily dispersed in the solvent (Figure S3, Supporting Information), forming a pseudohomogeneous reaction suspension with an extended two-dimensional structure. Thus, the reactive species can readily reach or leave the catalytic active sites with limited mass transfer resistance (Figure 8a). What is more, as illustrated in Figure 8b, the plierlike chelate ligands not only keep the planar steric structure of the copper complex but also increase the electron cloud density around the copper center. These characters further make for the smooth proceeding and excellent selectivity of the conversion process. In the meantime, the plierlike chelate structure also ensures the robust immobilization of copper complex onto the GO surface, which accounts for the remarkable reusability and stability of the immobilized catalyst.

4. CONCLUSIONS

In conclusion, we demonstrated an *in situ* strategy that a copper (salen) complex was synthesized and simultaneously immobilized onto GO support. The immobilized copper (salen) complex was demonstrated to be a highly effective and recyclable catalyst for the epoxidation of olefins. The excellent performance should owe to the outstanding properties of the GO support and the robust immobilization strategy. Herein, GO presents its unique advantages and potential in supporting homogeneous metal complexes for practical applications. The designed strategy is also readily extended to apply to other immobilization systems. More wide and in-depth

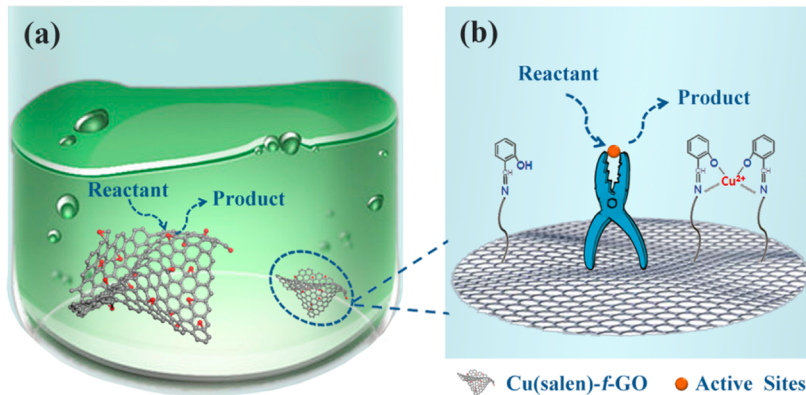


Figure 8. Illustration for (a) the mass transfer phenomenon in the reaction mixture and (b) the robust immobilization strategy.

applications in heterogeneous coordination catalysis are anticipated.

■ ASSOCIATED CONTENT

Supporting Information

The details of control experiments and supplementary figures. This material is available free of charge via the Internet at <http://pubs.acs.org>.

■ AUTHOR INFORMATION

Corresponding Author

*Phone: +86 22-27890090. E-mail: xiaobinfan@tju.edu.cn

Notes

The authors declare no competing financial interest.

■ ACKNOWLEDGMENTS

This study was supported by the National Natural Science Funds for Excellent Young Scholars (no. 21222608), Research Fund of the National Natural Science Foundation of China (no. 21106099), Foundation for the Author of National Excellent Doctoral Dissertation of China (no. 201251), the Tianjin Natural Science Foundation (no. 11JCYBJC01700) and the Programme of Introducing Talents of Discipline to Universities (no. B06006).

■ REFERENCES

- (1) Cole-Hamilton, D. J. Homogeneous Catalysis—New Approaches to Catalyst Separation, Recovery, and Recycling. *Science* **2003**, *299*, 1702.
- (2) Terry, T. J.; Stack, T. D. P. Covalent Heterogenization of a Discrete Mn(II) Bis-Phen Complex by a Metal-Template/Metal-Exchange Method: An Epoxidation Catalyst with Enhanced Reactivity. *J. Am. Chem. Soc.* **2008**, *130*, 4945.
- (3) Genna, D. T.; Wong-Foy, A. G.; Matzger, A. J.; Sanford, M. S. Heterogenization of Homogeneous Catalysts in Metal-Organic Frameworks via Cation Exchange. *J. Am. Chem. Soc.* **2013**, *135*, 10586.
- (4) Sheet, D.; Halder, P.; Paine, T. K. Enhanced Reactivity of a Biomimetic Iron(II) α -Keto Acid Complex through Immobilization on Functionalized Gold Nanoparticles. *Angew. Chem., Int. Ed.* **2013**, *52*, 13314.
- (5) Baleizão, C.; Garcia, H. Chiral Salen Complexes: An Overview to Recoverable and Reusable Homogeneous and Heterogeneous Catalysts. *Chem. Rev.* **2006**, *106*, 3987.
- (6) Vriamont, C.; Devillers, M.; Riant, O.; Hermans, S. A Covalently Anchored Homogeneous Gold Complex on Carbon Nanotubes: A Reusable Catalyst. *Chem. Commun.* **2013**, *49*, 10504.
- (7) Gupta, K. C.; Kumar Sutar, A.; Lin, C.-C. Polymer-Supported Schiff Base Complexes in Oxidation Reactions. *Coord. Chem. Rev.* **2009**, *293*, 1926.
- (8) Zhang, Y.; Riduan, S. N. Functional Porous Organic Polymers for Heterogeneous Catalysis. *Chem. Soc. Rev.* **2012**, *41*, 2083.
- (9) Oosterom, G. E.; Reek, J. N. H.; Kamer, P. C. J.; van Leeuwen, P. W. N. M. Transition Metal Catalysis Using Functionalized Dendrimers. *Angew. Chem., Int. Ed.* **2001**, *40*, 1828.
- (10) Yusuf, S.; Jiao, F. Effect of the Support on the Photocatalytic Water Oxidation Activity of Cobalt Oxide Nanoclusters. *ACS Catal.* **2012**, *2*, 2753.
- (11) Zhao, B.; Han, Z.; Ding, K. The N-H Functional Group in Organometallic Catalysis. *Angew. Chem., Int. Ed.* **2013**, *52*, 4744.
- (12) Geim, A. K.; Novoselov, K. S. The Rise of Graphene. *Nat. Mater.* **2007**, *6*, 183.
- (13) Chen, D.; Feng, H.; Li, J. Graphene Oxide: Preparation, Functionalization, and Electrochemical Applications. *Chem. Rev.* **2012**, *112*, 6027.
- (14) Dodoo-Arhin, D.; Fabiane, M.; Bello, A.; Manyala, N. Graphene: Synthesis, Transfer, and Characterization for Dye-Sensitized Solar Cells Applications. *Ind. Eng. Chem. Res.* **2013**, *52*, 14160.
- (15) Haddon, R. C. Graphene – The Mother of Two-Dimensional (2-D) Materials. *Acc. Chem. Res.* **2013**, *46*, 2191.
- (16) Scheuermann, G. M.; Rumi, L.; Steurer, P.; Bannwarth, W.; Mühlaupt, R. Palladium Nanoparticles on Graphite Oxide and Its Functionalized Graphene Derivatives as Highly Active Catalysts for the Suzuki–Miyaura Coupling Reaction. *J. Am. Chem. Soc.* **2009**, *131*, 8262.
- (17) Chen, X.; Wu, G.; Chen, J.; Chen, X.; Xie, Z.; Wang, X. Synthesis of “Clean” and Well-Dispersive Pd Nanoparticles with Excellent Electrocatalytic Property on Graphene Oxide. *J. Am. Chem. Soc.* **2011**, *133*, 3693.
- (18) Yao, Y.; Yang, Z.; Sun, H.; Wang, S. Hydrothermal Synthesis of Co₃O₄–Graphene for Heterogeneous Activation of Peroxymonosulfate for Decomposition of Phenol. *Ind. Eng. Chem. Res.* **2012**, *51*, 14958.
- (19) Liang, Y.; Li, Y.; Wang, H.; Zhou, J.; Wang, J.; Regier, T.; Dai, H. Co₃O₄ Nanocrystals on Graphene As a Synergistic Catalyst for Oxygen Reduction Reaction. *Nat. Mater.* **2011**, *10*, 780.
- (20) Fu, Y.; Xiong, P.; Chen, H.; Sun, X.; Wang, X. High Photocatalytic Activity of Magnetically Separable Manganese Ferrite–Graphene Heteroarchitectures. *Ind. Eng. Chem. Res.* **2012**, *51*, 725.
- (21) Li, Q.; Fan, F.; Wang, Y.; Feng, W.; Ji, P. Enzyme Immobilization on Carboxyl-Functionalized Graphene Oxide for Catalysis in Organic Solvent. *Ind. Eng. Chem. Res.* **2013**, *52*, 6343.
- (22) Georgakilas, V.; Otyepka, M.; Bourlinos, A. B.; Chandra, V.; Kim, N.; Kemp, K. C.; Hobza, P.; Zboril, R.; Kim, K. S. Functionalization of Graphene: Covalent and Non-Covalent Approaches, Derivatives and Applications. *Chem. Rev.* **2012**, *112*, 6156.

- (23) Guo, Y.; Bao, C.; Song, L.; Yuan, B.; Hu, Y. In Situ Polymerization of Graphene, Graphite Oxide, and Functionalized Graphite Oxide into Epoxy Resin and Comparison Study of On-the-Flame Behavior. *Ind. Eng. Chem. Res.* **2011**, *50*, 7772.
- (24) Su, C.; Loh, K. P. Carbocatalysts: Graphene Oxide and Its Derivatives. *Acc. Chem. Res.* **2012**, *46*, 2275.
- (25) Yang, Q.; Pan, X.; Clarke, K.; Li, K. Covalent Functionalization of Graphene with Polysaccharides. *Ind. Eng. Chem. Res.* **2011**, *51*, 310.
- (26) Quintana, M.; Vazquez, E.; Prato, M. Organic Functionalization of Graphene in Dispersions. *Acc. Chem. Res.* **2013**, *46*, 138.
- (27) Zhao, Q.; Chen, D.; Li, Y.; Zhang, G.; Zhang, F.; Fan, X. Rhodium Complex Immobilized on Graphene Oxide As an Efficient and Recyclable Catalyst for Hydrogenation of Cyclohexene. *Nanoscale* **2013**, *5*, 882.
- (28) Hummers, W. S.; Offeman, R. E. Preparation of Graphitic Oxide. *J. Am. Chem. Soc.* **1958**, *80*, 1339.
- (29) Hemraj-Benny, T.; Wong, S. S. Silylation of Single-Walled Carbon Nanotubes. *Chem. Mater.* **2006**, *18*, 4827.
- (30) Ou, J.; Wang, J.; Liu, S.; Mu, B.; Ren, J.; Wang, H.; Yang, S. Tribology Study of Reduced Graphene Oxide Sheets on Silicon Substrate Synthesized via Covalent Assembly. *Langmuir* **2010**, *26*, 15830.
- (31) Ou, X.; Jiang, L.; Chen, P.; Zhu, M.; Hu, W.; Liu, M.; Zhu, J.; Ju, H. Highly Stable Graphene-Based Multilayer Films Immobilized via Covalent Bonds and Their Applications in Organic Field-Effect Transistors. *Adv. Funct. Mater.* **2013**, *23*, 2422.
- (32) Bhadbhade, M. M.; Srinivas, D. Effects on Molecular Association, Chelate Conformation, and Reactivity toward Substitution in Copper Cu(5-X-salen) Complexes, salen2- = N,N'-ethylenebis(salicylideneamino), X = H, CH₃O, and Cl: Synthesis, X-ray Structures, and EPR Investigations. *Inorg. Chem.* **1993**, *32*, 5458.
- (33) Kim, S.; Zhou, S.; Hu, Y.; Acik, M.; Chabal, Y. J.; Berger, C.; de Heer, W.; Bongiorno, A.; Riedo, E. Room-Temperature Metastability of Multilayer Graphene Oxide Films. *Nat. Mater.* **2012**, *11*, 544.
- (34) Ma, P. C.; Kim, J.-K.; Tang, B. Z. Functionalization of Carbon Nanotubes Using a Silane Coupling Agent. *Carbon* **2006**, *44*, 3232.
- (35) Kannari, N.; Ozaki, J.-i. Formation of Uniformly and Finely Dispersed Nanoshells by Carbonization of Cobalt-Coordinated Oxine—Formaldehyde Resin and Their Electrochemical Oxygen Reduction Activity. *Carbon* **2012**, *50*, 2941.
- (36) Zhao, Z.-P.; Li, M.-S.; Zhang, J.-Y.; Li, H.-N.; Zhu, P.-P.; Liu, W.-F. New Chiral Catalytic Membranes Created by Coupling UV-Photografting with Covalent Immobilization of Salen—Co(III) for Hydrolytic Kinetic Resolution of Racemic Epichlorohydrin. *Ind. Eng. Chem. Res.* **2012**, *51*, 9531.
- (37) Zude, Z.; Xiong, Z.; Tao, Z.; Huaming, Y.; Qingliang, L. Structural Study of Compartmental Complexes of Europium and Copper. *J. Mol. Struct.* **1999**, *478*, 23.
- (38) Ferrari, A. C.; Meyer, J. C.; Scardaci, V.; Casiraghi, C.; Lazzeri, M.; Mauri, F.; Piscanec, S.; Jiang, D.; Novoselov, K. S.; Roth, S.; Geim, A. K. Raman Spectrum of Graphene and Graphene Layers. *Phys. Rev. Lett.* **2006**, *97*, 187401.
- (39) Fang, M.; Wang, K.; Lu, H.; Yang, Y.; Nutt, S. Single-Layer Graphene Nanosheets with Controlled Grafting of Polymer Chains. *J. Mater. Chem.* **2010**, *20*, 1982.
- (40) Fang, M.; Wang, K.; Lu, H.; Yang, Y.; Nutt, S. Covalent Polymer Functionalization of Graphene Nanosheets and Mechanical Properties of Composites. *J. Mater. Chem.* **2009**, *19*, 7098.
- (41) Manna, A. K.; Pati, S. K. Tuning the Electronic Structure of Graphene by Molecular Charge Transfer: A Computational Study. *Chem. — Asian J.* **2009**, *4*, 855.
- (42) Rao, C. N. R.; Sood, A. K.; Voggu, R.; Subrahmanyam, K. S. Some Novel Attributes of Graphene. *J. Phys. Chem. Lett.* **2010**, *1*, 572.
- (43) Silva, A. R.; Freitas, M. M. A.; Freire, C.; de Castro, B.; Figueiredo, J. L. Heterogenization of a Functionalized Copper(II) Schiff Base Complex by Direct Immobilization onto an Oxidized Activated Carbon. *Langmuir* **2002**, *18*, 8017.
- (44) Pratt, R. C.; Lyons, C. T.; Wasinger, E. C.; Stack, T. D. P. Electrochemical and Spectroscopic Effects of Mixed Substituents in Bis(phenolate)-Copper(II) Galactose Oxidase Model Complexes. *J. Am. Chem. Soc.* **2012**, *134*, 7367.
- (45) Ji, J.; Zhang, G.; Chen, H.; Wang, S.; Zhang, G.; Zhang, F.; Fan, X. Sulfonated Graphene As Water-Tolerant Solid Acid Catalyst. *Chem. Sci.* **2011**, *2*, 484.
- (46) Fraile, J. M.; Garcia, J. I.; Herreras, C. I.; Mayoral, J. A.; Pires, E. Enantioselective Catalysis with Chiral Complexes Immobilized on Nanostructured Supports. *Chem. Soc. Rev.* **2009**, *38*, 695.
- (47) Wegener, S. L.; Marks, T. J.; Stair, P. C. Design Strategies for the Molecular Level Synthesis of Supported Catalysts. *Acc. Chem. Res.* **2012**, *45*, 206.
- (48) Nakazawa, J.; Smith, B. J.; Stack, T. D. P. Discrete Complexes Immobilized onto Click-SBA-15 Silica: Controllable Loadings and the Impact of Surface Coverage on Catalysis. *J. Am. Chem. Soc.* **2012**, *134*, 2750.